Sedighi *et al.*
Journal of Engineering and Applied Science (2022) 69:58
https://doi.org/10.1186/s44147-022-00110-7

Journal of Engineering and Applied Science

RESEARCH Open Access

Experimental investigation of flow pattern at 180° bend with rigid bed in effect of twin convergent bridge piers

Farid Sedighi, Mohammad Vaghefi* and Elham Zarei

*Correspondence: Vaghefi@pgu.ac.ir

Department of Civil Engineering, Persian Gulf University, Shahid Mahini St, Bushehr 7516913817, Iran

Abstract

The generation of vortices in sharp bends of rivers is a well-known phenomenon. However, their influence on the bridge pier has not been investigated deeply. This study studies the flow pattern around the twin convergent bridge pier in a sharp bend by an experimental approach. The test facility includes a channel located at Advanced Hydraulic Laboratory, Persian Gulf University, with a 1 m width and 2 m central radius. The flow 3D velocity is measured along the bend by an ADV velocimeter. It is realized that the most important vortex from a sediment transport point of view is located adjacent to a pier in a plane just parallel to the flow direction. Furthermore, it could be concluded that the pier influencing range has an approximate dimension of 10 times pier diameter in a plane parallel to flow and 3 timer pier diameters in the vertical plane. Results and discussions are presented throughout the paper.

Keywords: ADV, Bend, Flow pattern, Streamline, Twin convergent bridge piers

Introduction

Bridges and their piers are regarded as one of the oldest riverine structures used by humankind. Different types of piers are used in the construction of bridges. In most cases, according to regional restrictions, engineers have to construct bridges on bending paths of rivers.

For years, the complicated flow pattern in river bends has challenged the river engineers. Secondary flows, flow attack to the outer bank, the helical motion of flow in the bend, etc., are among few differences of stream in bends compared to straight paths. There are different ways of flow capturing. For example, injection of colored particles and image processing through computer programs or 2D velocimetry could be applied for flow pattern capturing. In the current research, the ADV velocimeter, manufactured by NORTEK, is utilized to measure flow velocity in three dimensions at a sample rate of 25 Hz. Some innovations of this research include flow pattern recognition around twin convergent piers and sharp 180° bend in the channel. Few scientific reports concentrate on flow patterns around bridge piers in contrast to several contributions to scouring, mainly because of expensive instrumentation and

time-consuming experiments. Pioneers of precise flow pattern recognition go back to 1994 by ADV velocimeter of SonTek. Anderson and Lohrmann [4] compared measurements by ADV velocimeter to older samples recorded by Vector Averaging Current Meter (VCMC) through experiments. Measurements showed acceptable precision and proved the performance of ADV sensors. Sarker [30] applied the same velocimeter to study the flow pattern around a cylindrical bridge pier in a channel with a straight test section with a width of 90 cm. The generation of an artificial wave in the channel was significant in this research. Ahmed and Rajaratnam [1] performed three types of tests: flow pattern test on the rigid bed, flow pattern on the rough bed, and finally, flow pattern and scouring test on the live bed. The effects of roughness on bed stress and flow pattern on scour depth are determined by comparing these three individual experiments. Several studies have focused on the flow pattern in bends. Blanckaert and Graf [10] concluded that the turbulence structure in a bend was different from that in a straight flow, most notably in reducing the turbulent activity toward the outer bank. Graf and Istiarto [20] calibrated an ADVP velocimeter to study the flow pattern around the cylindrical bridge pier on a live-bed, and vortices were documented. Barbhuiya and Dey [8] focused on the flow pattern around bridge abutment. According to the experiments, bed shear stress could increase up to 3.3 times initial stress. Salajegheh et al. [29] studied the flow pattern in a 180° bend of a gradually increasing water channel and analyzed the transverse flows. The channel bed was considered rigid without any obstacles. Naji Abhari et al. [26] investigated the flow pattern in 90° bend through experiments and numerical simulations. A comparison of hydraulic parameters reveals that the software models the bend accurately. Kumar et al. [22] studied the flow characteristics around a bridge pier equipped with the collar on a live-bed. The influences of the collar on the horseshoe vortex around the pier and its consequent scouring were reported. Ataie-Ashtiani and Aslani-Kordkandi [6] studied the twin vertical cylindrical pier in a straight channel. Experiments were repeated for two cases of live and rigid beds. The velocity and shear stress were magnified in the region trapped by the pier. Ataie-Ashtiani and Aslani-Kordkandi [7] focused on the flow pattern around single and twin cylindrical type piers located in a flow parallel plane. According to the experiment, velocity declines significantly while approaching the bed, and the streamlines were quite different around the pier located downstream. ADV velocimeter was used to capture the flow pattern. Das et al. [15] considered the twin pier in the flow parallel plane. Flow hydraulic parameters were calculated, and a graphical illustration of streamlines visualized horseshoe vortices. Vaghefi et al. [36] measured velocity contours in sharp bends through experiments with an ADV velocimeter. The flow velocity in different layers was measured, and streamlines were visualized. Vaghefi et al. [34, 35] experimented with a flow pattern in a 180° bend. It was demonstrated that maximum shear stress occurs at an angle equal to 40° from the bend start-point, and maximum secondary flow strength occurred at the bend's second half. Vaghefi et al. [37, 38] studied scouring patterns around a single inclined pier in a straight channel. They observed that the pier inclinations in the flow parallel plane did not affect the scour hole depth around it. Meanwhile, any inclination in the parallel flow plane would result in higher scouring levels. Pier geometry and its configuration with respect to flow can influence flow patterns

downstream and, consequently, scouring depth. Fael et al. [18] studied the effect of shape on scouring depth experimentally. According to the results, shape factors calculated based on short experiments can be assumed to be constant. Yilmaz et al. [42] developed a semi-empirical model to estimate the temporal variation of scour depth around cylindrical piers arranged in tandem. They also proposed a relation between dimensionless scour depth and time. Dey et al. [17] analyzed flow wake in downstream of a vertical cylinder experimentally. Vecterino velocimeter is utilized to measure the flow profile. Guan et al. [21] used the PIV method to capture the flow pattern around cylindrical piers. They realized that the size of the main vortex depends extremely on the scour depth. Wang et al. [41] conducted systematic experiments to study the interactions of circular piers and downstream structures such as weirs. It was found that downstream structures could be very beneficial in reducing the scour on piers. Liu et al. [24] conducted 95 tests to observe the effects of the pier spacing, and the flow velocity on the local scour development of the twin piers. Das and Mazumdar [16] presented experimental results of mean and turbulent flow parameters around two square piers. They concluded that horseshoe vortex strength for the eccentric-rear pier was greater than the strength for the inline-front pier. Gauton et al. [19] compared flow patterns around complex piers to single piers. Applying complex piers could eliminate the vortexes generated around the pier. Chooplou and Vaghefi [13] studied velocity and bed shear stress distribution in 180° bend around bridge pier and submerged vanes. Vijayasree et al. [40] investigated the flow field experimentally, and the local scour around bridge pier of different shapes on a sediment bed. Asadollahi et al. [5] compared flow and scour patterns around a single and triple bridge pier experimentally and numerically at a 180° sharp bend. Lee and Hong [23] conducted hydraulic laboratory experiments in a rectangular flume to understand near-bed turbulence characteristics. The results of velocity measurements upstream of the pier in the horseshoe vortex region showed significant differences before and after scouring. Carnacina et al. [12] analyzed the rate of scour temporal evolution, the average three-dimensional flow velocities, turbulence intensities, Reynold stress, and turbulent kinetic energy around a cylindrical bridge pier. Velocity measurements were taken using a Nortek acoustic Velocimeter at 25 Hz. Das et al. [14] investigated a relative scour condition around a three-pier group using a number of laboratory-scale experiments. They proposed scour depth equations around individual piers of the pier group according to the spacing between the piers arranged in tandem. Sedighi et al. [31] performed three separate experiments under clear water and movable bed conditions to study the effects of inclined pair piers on bed topography in a scaled river bend. Vijayasree et al. [39] studied turbulence characteristics such as mean velocities, Reynolds stresses, and turbulent kinetic energy along the oblong and the circular piers in a laboratory flume. Moghanloo and Vaghefi [25] investigated the collar's effect on the flow pattern around an oblong pier in bend experimentally. The results suggested that with an increase in the thickness of the collar, the tendency of the upstream streamlines toward the inner bank increased. Behrouzi et al. [9] simulated flow patterns and turbulent kinetic energy around single and twin bridge piers using Fluent. They recommended the side-by-side model as the most appropriate arrangement of the piers regarding the flow direction.

Methods

The water channel of Advanced Hydraulic Research Laboratory, Persian Gulf University, is used for the experimental purposes of this research. A 180° bend channel with the central radius (Rc) = 2 m and the width (B) = 1m (Rc/B = 2) is considered sharp [11]. The channel has a straight inlet path stretched by 6.5 m when approaching the bend and 5.1 m leaving the bend. A gate is located at the end of the channel for adjustment of water depth. Passing through the gate, water enters a tank arranged just below the channel. Pumps, inlet and outlet pipes, and tanks have no direct touch with the channel to avoid any unintended vibrations on the channel structure. The channel overview is shown in Fig. 1.

Vectrino velocimeter, manufactured by NORTEK, is applied for 3D velocimetry. High precision compared to similar instruments, hydrodynamic design of probe to reduce the oscillations in flow field are named as advantages of the instrument. In addition, four-receiver gauges provide more accurate measurements, especially in highly oscillating unsteady flows. Side and bottom-looking probes are applied in the current experiments. Measured data is analyzed by ExploreV software. Different filtering and averaging algorithms are applied in the signal processing stage. A convergent twin pier under 21° relative to the vertical line is considered here [38]. PVC in 50 mm diameter manufactures the piers. Figure 2 represents the piers and their configuration. The piers are located at the 90° cross section. Therefore, the cross sections before the apex of the bend are upstream, and thereafter, they are considered downstream. A 1.5 mm diameter thin layer of material is sticked to the channel bed to simulate natural roughness. This is selected according to Raudkivi and Ettema's [28] recommendation to prevent formation of ripples (the diameter of the material should not be less than 0.7 mm). The flow rate was set at 70 L/s, and the depth was set to 18 cm. Hence, the flow velocity to critical velocity ratio is 0.98 [27]. The Froude number is considered 0.29. The flow domain in the channel is discretized for velocimetry. Mesh size is refined in the regions where large turbulence and

Fig. 1 Experimental channel in Persian Gulf University

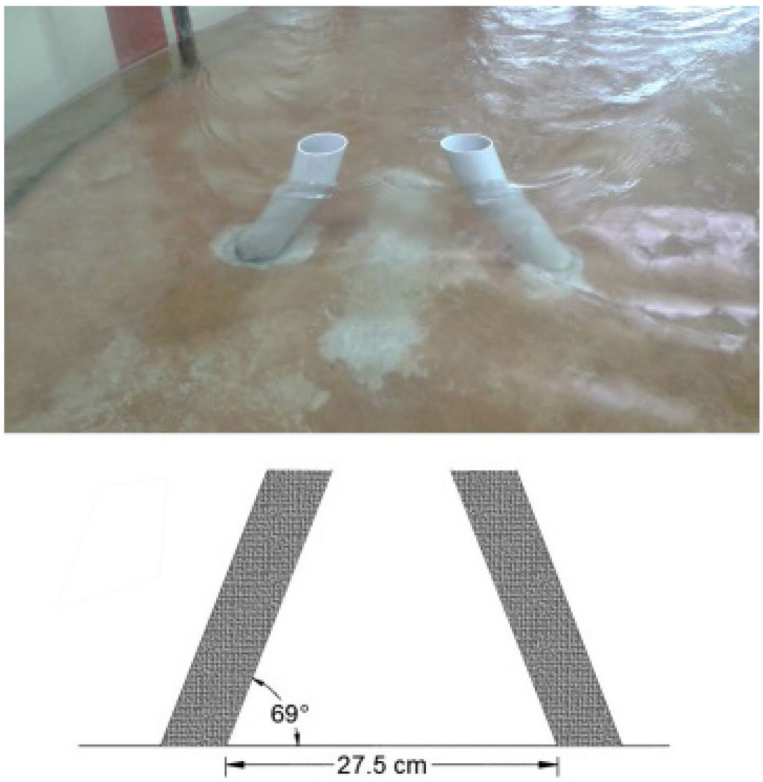

Fig. 2 Convergent pier during experiments and general arrangement

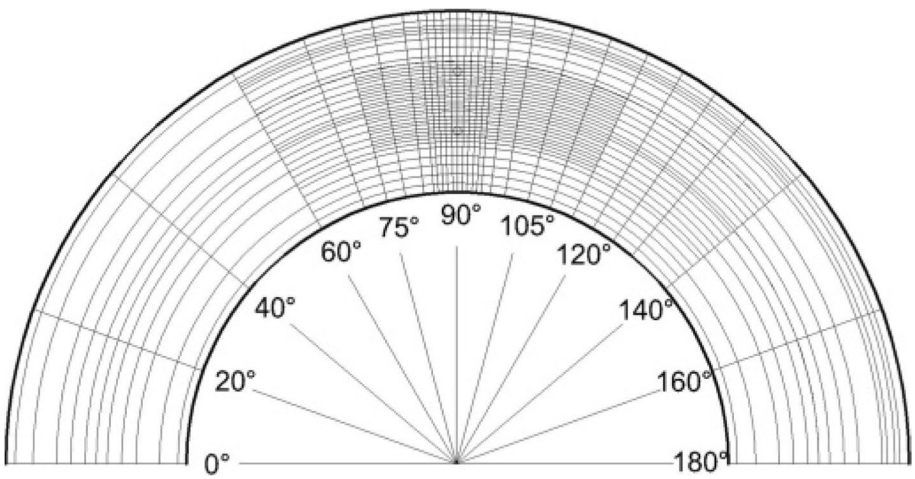

Fig. 3 Velocimetry grid at depth level equal to 6% of the total depth (measured from the bed)

oscillations of fluid flow are expected. The smallest size of the grid has been 1° in angle and 2 cm for changes in the transverse direction. Measurements are performed in 6 different level depths. The recording points in each depth would be different because of the inclination of the piers. Figures 3 and 4 describe the flow measurement grids. Level depths for three-dimensional flow measurements are 1, 3, 7, 11, 14, and 18 cm from the channel bed.

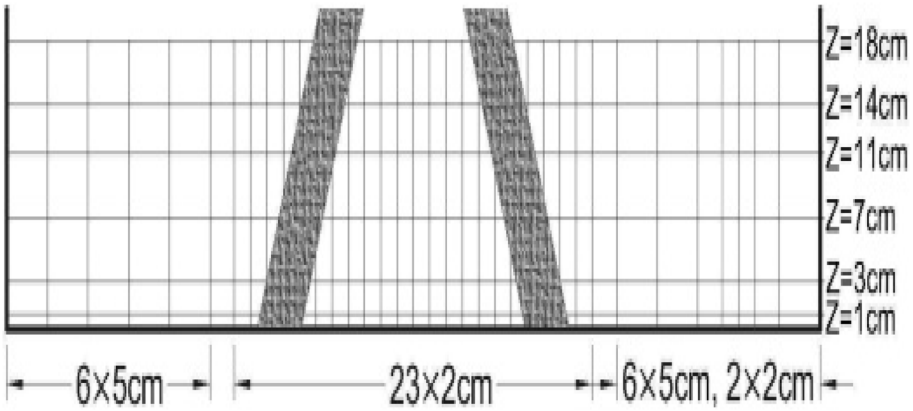

Fig. 4 Velocimetry grid cross section in 90°

Results and discussions

Transverse and longitudinal sections and the plan views are studied in this paper. Tangential, lateral, and vertical velocity components are plotted in different profiles. Moreover, to enhance the accuracy of flow capturing, parameters such as secondary flow and vorticity are calculated, and all the characteristics are compared.

Transverse sections

Flow velocity in straight-line paths follows a logarithmic profile. Lateral velocity is negligible, and no vortex or secondary flow is observed in this direction. However, it would be completely the other way for flow in bends. Fluid flow through a bend results in a centrifugal force, and the water elevates on the outer side of the bend. This change imposes a pressure gradient and differences in flow potential. Consequently, secondary flows would be inevitable. In such circumstances, a main secondary flow is generated that is dominant in the whole curved path of the fluid. Streamlines in cross sections are represented in Fig. 5. The horizontal axis represents the distance to the inner bank (B) in centimeters, and the vertical axis represents the distance to the channel bottom (Z) in centimeters. Secondary flows are quite apparent in these sections. Secondary flows are fully developed from an angle of 20° and would be dominant along the channel up to the end. According to the channel shape, the flow rotates clockwise towards the end of the bend, so called helical flow. Main secondary flow moves from the outer bend through the inner bend in lower depth levels and from the inner bend through the outer bend for upper depth levels, despite the bend's entrance portion that contradicts behavior. The transverse component of velocity in the whole section is very small (around 2 to 3 cm/s) towards the inner bank. The main reason could be the variations of the path through the channel. Overall, the flow tends to follow the same path as a channel; however, the centrifugal force is not generated completely, and flow circulation cannot be observed completely.

In most cases, the main secondary flow is observed in the inner bend as a vortex. Flow transverse velocity in layers near the channel bed is 50 to 100% higher than in upper layers. Hence, the flow deviates towards the lower layers before encountering the outer

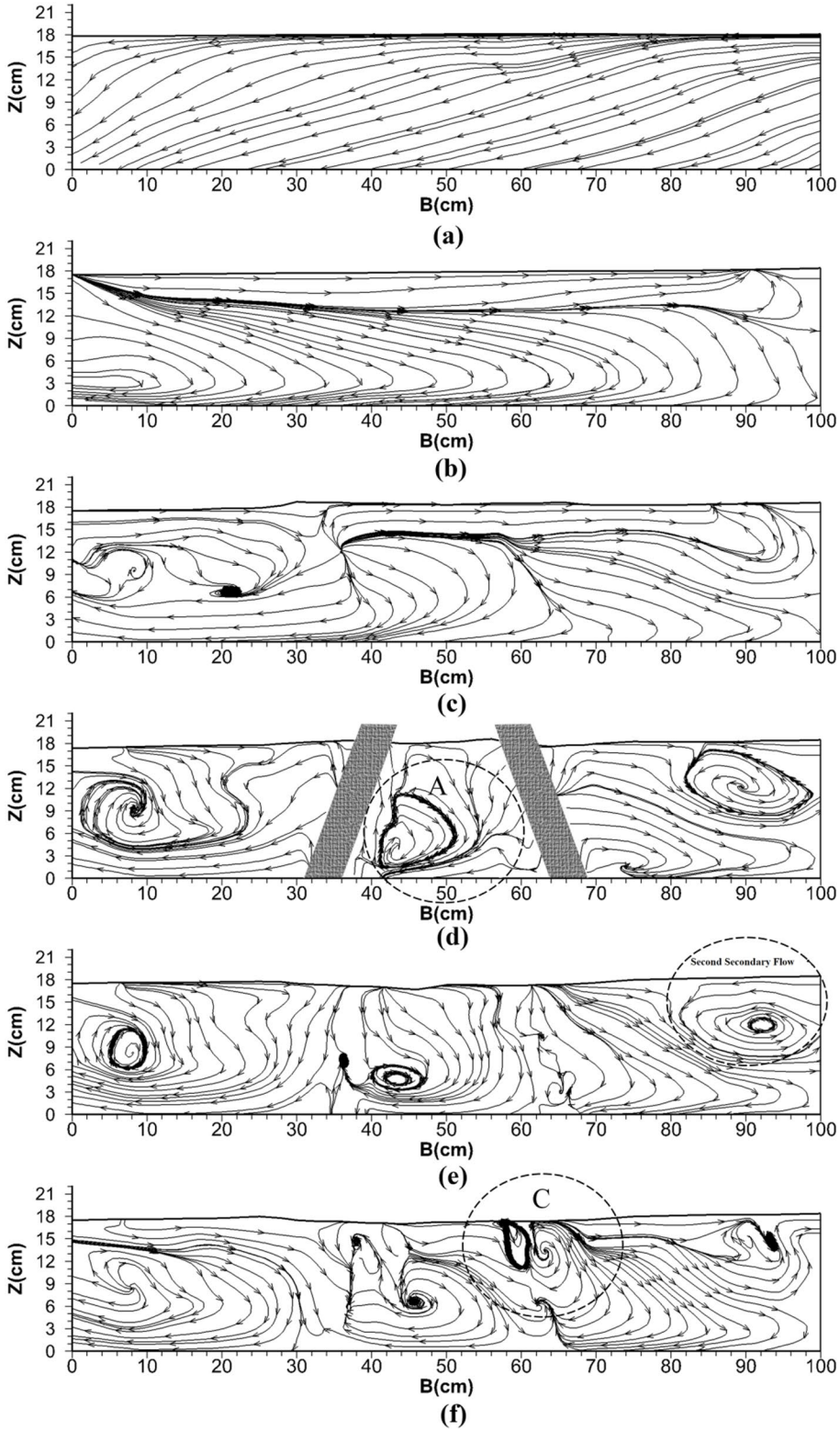

Fig. 5 Streamlines in transverse cross sections (**a)** 0, (**b)** 40, (**c)** 88, (**d)** 90, (**e)** 91, (**f)** 97° from the beginning of the bend

wall, and the vortex is observed in the inner bend. This vortex would be apparent even in the first angles of the bend. It could be claimed that this. Type of flow is the main flow observed in 65% of transverse cross-sections. Therefore, it is called the main secondary flow. This vortex is shown evidently in Fig. 5b. As aforementioned, another secondary flow starts at an angle of 60°. This flow depends highly on shape and type of bend and would be observable just in some limited angles. This flow is called "second secondary flow". The second secondary flow direction is opposite to the main secondary flow. This type of flow is most probable in sharp bends. It should be emphasized that the presence of a pier or any other obstacles does not influence the generation of this flow. This flow is reported to be at an angle near 45° for 90° bends by flow pattern studies Vaghefi et al. [36]. Furthermore, Blanckaert and Graf [10] studied the flow pattern in 120° bends and reported the occurrence angle of second secondary flow around 60°, measured from the starting point of the bend.

According to the results, at an angle of around 80° from the beginning of the bend, a small-sized vortex is generated near the inner bank, which counteracts the main secondary flow. This vortex covers 20% of the total channel width from the inner bank. The vortex developed even adjacent to piers and vanished afterward. Similarly, two vortices of the same shape and at the same location are observed during the experiments in the cross section located at 85°. Generally, the flow pattern does not experience significant changes compared to previous cross sections. Even patterns of second secondary flow around the outer bend represent the same behavior and cover 80 to 100% of the channel width. Some oscillations are observed in the opposite direction to the main secondary flow. These oscillations could be regarded as the initial pulses of a vortex generated due to an obstacle to fluid flow and contraction in the section. This vortex is observable at 89° and maintains its shape until the angle is 149°. Afterward, it gradually loses energy and rearranges in the flow direction.

The second secondary flow is responsible for 5 to 6% of the total flow area, and it is located near the outer wall. Thus, it has negligible effects on scouring and stresses around the pier. The first influences of the pier of flow pattern are recorded at around 87°. However, the variations in flow patterns are very slight, and it is sensible only through a three-dimensional analysis of flow velocity rate. According to the experiments in 88°, variations in flow patterns are rather apparent, and a dramatic change in flow direction is reported in the center of the channel. From this angle, flow begins to divide into two portions on 40 to 60% channel width and separates the ways from the main secondary flow. This flow separation is mainly due to the piers installed in 90° section. According to the significant influences of the pier at 88°, it could be concluded that piers influence the flow pattern in upstream in a region designated to a diameter of 1.5 times pier diameter.

The mentioned trends in flow patterns are very influential in scouring bridge piers. Considering the experimentations with live beds, these flows can be categorized as downstream flows causing scouring. When downstream flows encounter the materials on the bed, there is a possibility that they lift the materials and wash them downstream through the main flow. Downstream-directed streamlines were not reported in channel center only at the location of the piers (90°), and a single vortex could be generated between twin piers due to an encounter with an obstacle. The distance between the

center of this vortex to the pier, nearer to the inner bend, is smaller. This phenomenon is mainly a result of the larger secondary flow velocity at layers closer to the bed, and as it was mentioned earlier, they are oriented toward the outer wall. Therefore, it attracts the generated vortex towards the first pier. This is the most responsible vortex for damages to the bed around the pier. Vortex (*C*), as shown in Fig. 5, Vortex (*C*) is one of the vortices that rotate in the opposite direction, and it is demonstrated in Fig. 5 that this vortex vanishes downstream. This vortex is captured only in the section located at 97° from the bend beginning. Special attention should be drawn to tangential velocities in studying the vortices above. It is demonstrated that some vortices downstream of the pier experience negative tangential velocities that indicate the reverse flows. These flows create some vortices that can be captured through the three-dimensional analysis of flow deviation. The tangential velocity contour is represented in Fig. 6. This section is located at 91°, just adjacent to downstream of the piers.

It should be emphasized that the generated vortices move toward the channel downstream spirally due to variations of transverse velocity at different depth levels. For illustration, the distribution of transverse velocity is presented in Fig. 7, and the vertical distribution of flow velocity in sections 89, 90, and 91° are compared in Fig. 8. According to the diagrams, when approaching the bed, flow is toward the inner bank and is reversed on the free surface. Moreover, due to the obstacle facing the flow, vertical velocity values in 90° locations (that is, the location considered for inclined pier installation) show considerable changes. If a vortex is generated in a parallel plane to flow, this velocity difference in adjacent layers will result in the spiral motion of the vortex.

According to the experiments, the channel width could be divided into three distinct portions. The first portion is located in 0 to 30% of channel width (referenced to the inner bank) large irrotational flow is recorded that is the main secondary flow in bending paths. The type of flow path is responsible for the creation of this flow. Second, a new region is identified, located in 30 to 70% of the channel width that occurs because of an obstacle (bridge pier in this case) against the flow. Large turbulence and oscillations are observed in this region, and the flow pattern alters rapidly. In some sections of this portion, vortices are generated. Some of these vortices vanish in the

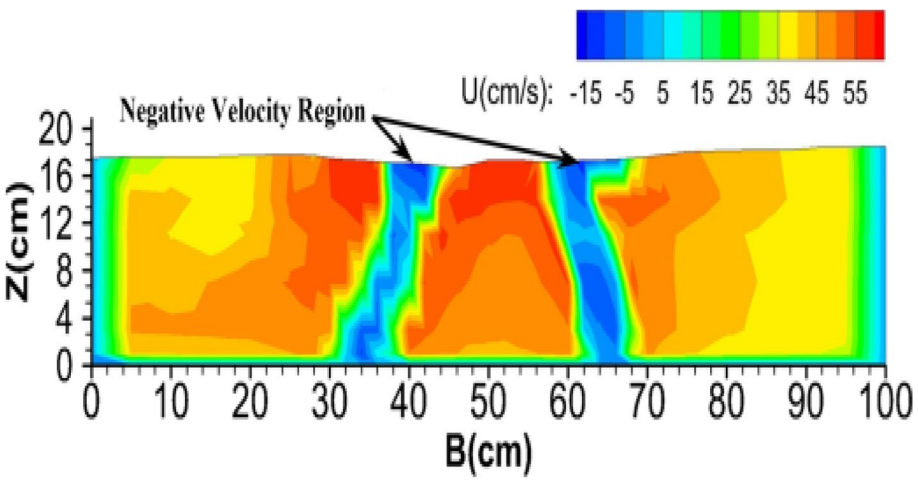

Fig. 6 Tangential velocity contours on cross section located at 91°

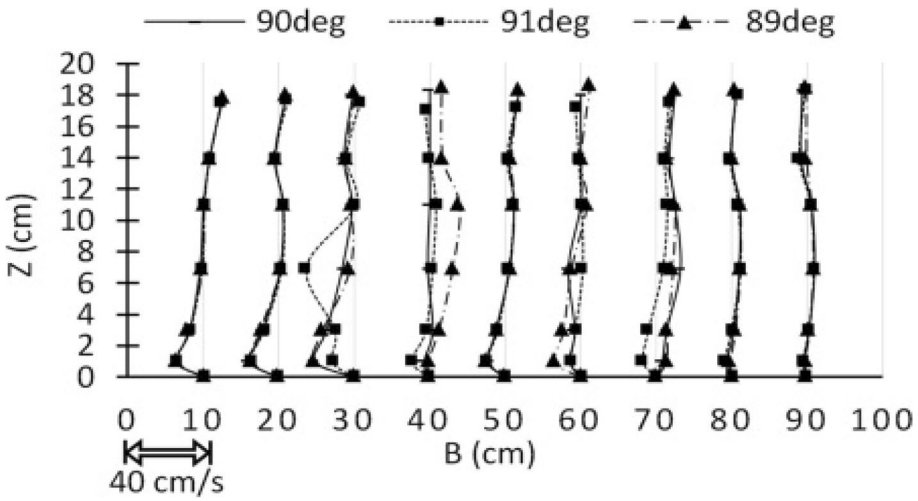

Fig. 7 Comparison of transverse velocities in locations 89, 90, and 91° of bent path

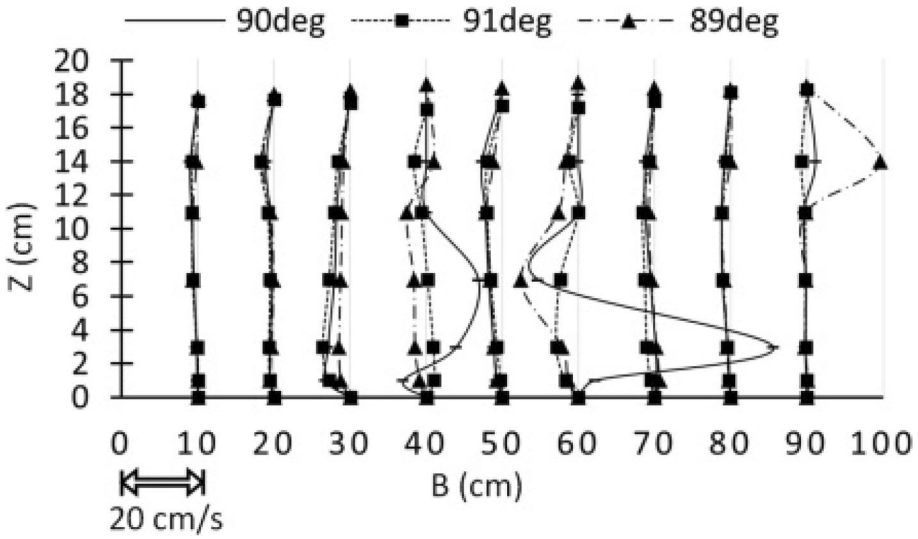

Fig. 8 Distribution of vertical velocity in locations 89, 90, and 91° of bent path

next cross sections, and some amplify. This region could be regarded as a "destructive region". The third portion is located at one-third width of the channel from the end. This region is identified by 70 to 100% of the channel width from the inner bank. The main cause of vortex generation in this region is the bended path. This vortex opposes the main secondary flow, which is called second secondary flow, discussed briefly in the previous. This classification is valid from 88 to 130° from the beginning of the bend and for a distinct region of 2 times the pier diameter towards upstream and 25 times pier diameter towards downstream. After that, the fluid flow enters into transition. Turbulence is generated due to the pier weakening, and the main free stream starts to appear gradually. These variations are rather slight and occur at 40° of the bend, corresponding to 30 times the pier diameter.

Longitudinal sections

Several vortices are recorded by measurements of flow patterns in longitudinal profiles of the channel. These vortices are mainly parallel to flow direction. Longitudinal sections and corresponding streamlines are illustrated in Fig. 9. The vertical axis represents the distance to the channel bed in centimeter, while the horizontal axis represents the position from the beginning of the bend in degrees. The first influences of piers on flow patterns are recorded at 32% of channel width from the inner bank. It is worth noting that piers are expressed as ellipses in each section due to the inclination of piers concerning normal direction. A small reverse flow was recorded downstream of piers through analysis of velocity contours.

As an example, A's region in Fig. 9c represents the reverse flow that is captured as a spiral vortex in the three-dimensional analysis. The distribution of tangential velocity in longitudinal sections at distances located at distances of 47, 50, and 57 cm from the inner bank is represented in Fig. 10. Realizing the negative tangential velocities adjacent to piers, vortex generation would be inevitable. No considerable influence

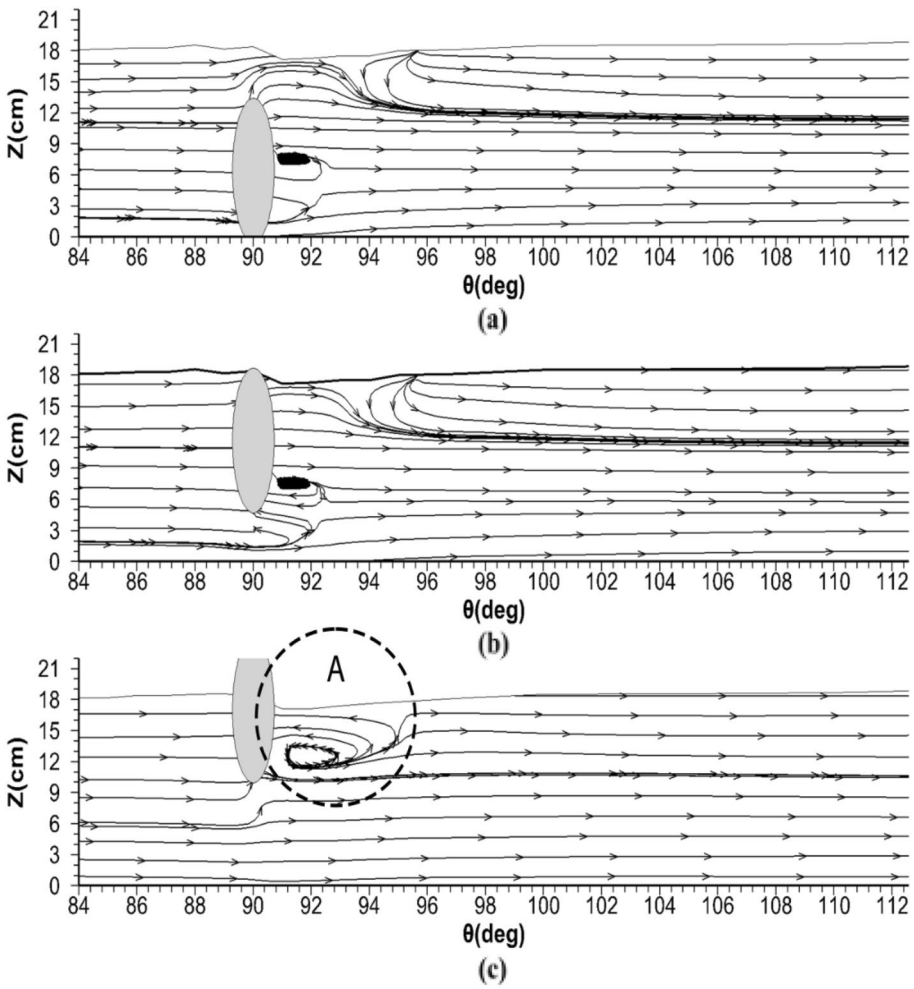

Fig. 9 Longitudinal sections in (**a**) 36%, (**b**) 38%, (**c**) 40% of channel width from inner bank

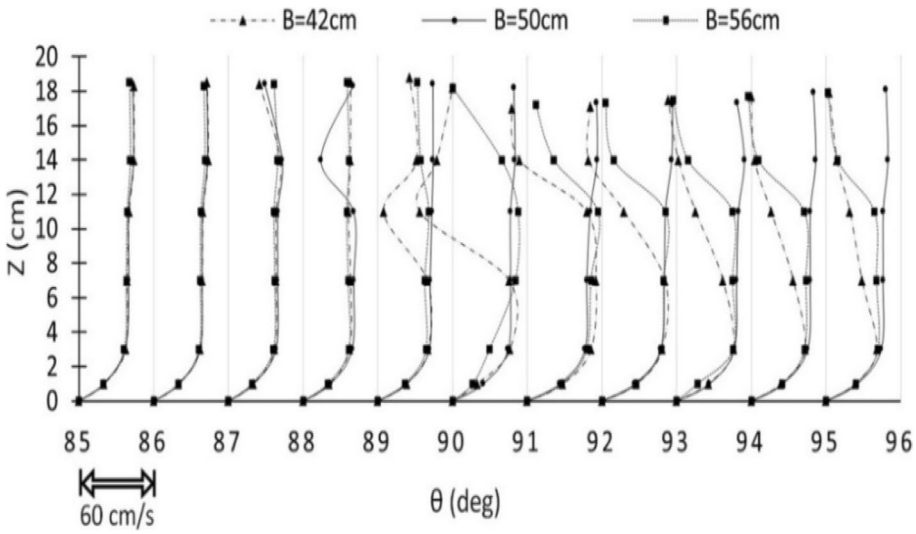

Fig. 10 Distribution of tangential velocity in 42%, 50%, and 56% of channel width from inner bank

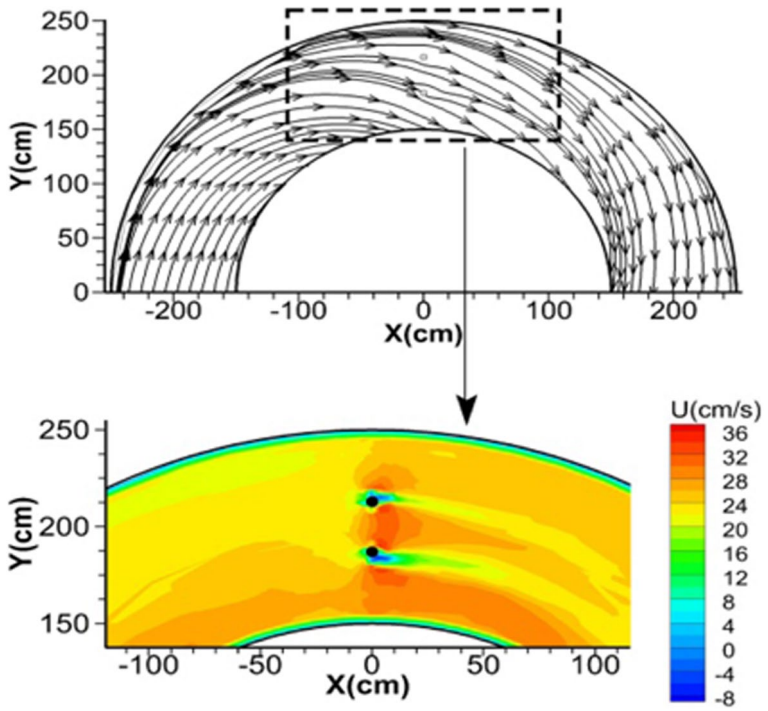

Fig. 11 Streamlines and tangential velocity contours in 6% depth from channel bed (magnified)

is reported in longitudinal sections between two legs. However, analysis of velocity contour reveals the increase of tangential velocity due to contraction of the section.

Flow analysis in plan view

Streamlines and tangential velocity contour in 6% depth are represented in Fig. 11. Negative tangential velocities and deviation of streamlines are quite clear. Analysis of

sections in different levels reveals that the flow tends toward the inner bank in deeper layers. Meanwhile, in upper levels, the stream deviates through the outer bank. Similar changes have been reported in 180° sharp bends without structures [35] and in 180° sharp bends with T-shaped spur dikes [3].

Considering the three-dimensional characteristics of flow and changes in streamline levels, one can imagine the spiral motion of the flow. Considering the two mentioned levels, the angle between streamlines would be around 22°. Guidance for measurement of streamline deviations relative to the original path is represented in Fig. 12. Different levels' deviation is calculated, and offsets are presented in Fig. 13. According to Fig. 13b, maximum stream deviation has occurred at an angle equal to 70 to 80° from the beginning of the bend.

To create a better comparison between streams at different levels, the paths of maximum tangential velocity are given in Fig. 14. According to Fig. 14, the maximum values of tangential velocities on deeper levels and upper levels differ significantly. Moreover, it is affected by the pressure gradient due to the bending shape of the passage. The maximum velocity at the end of the bend occurs on the outer bank for both levels. Meanwhile, it is not true for the center of the bend. These pieces of evidence demonstrate that flow tends to deflect towards the outer bank due to centrifugal forces. However, the generation of secondary flow prevents this effect completely. This trend in the 180° sharp bend without a pier has also been reported by Akbari and Vaghefi [2].

Another observed phenomenon during experiments is horizontal vortices in the XY plane. Maximum intensities of these vortices occur on the largest level while it appears at all levels. To make the best prediction for the probability of vortex generation, tangential velocity contour is applied in magnified plans. This contour is dark for negative tangential velocity regions (reverse flows). Reverse flow is an influencing factor in vortex generation. According to drawn plans, the maximum influence of piers on vortex generation occurs in the range limited by 4 times of pier diameter.

The tangential velocity has a more negative value at upper levels of the flow and downstream of the piers. Considering the three-dimensional characteristics of the flow and

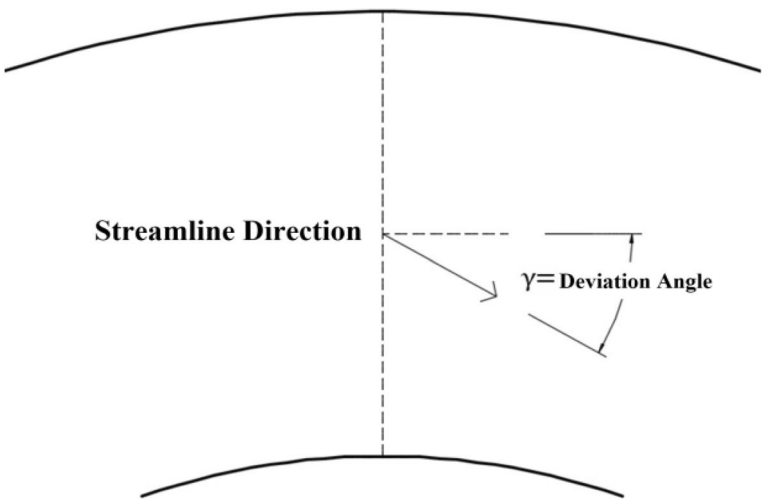

Fig. 12 Guidance for measurement of stream deviation angle

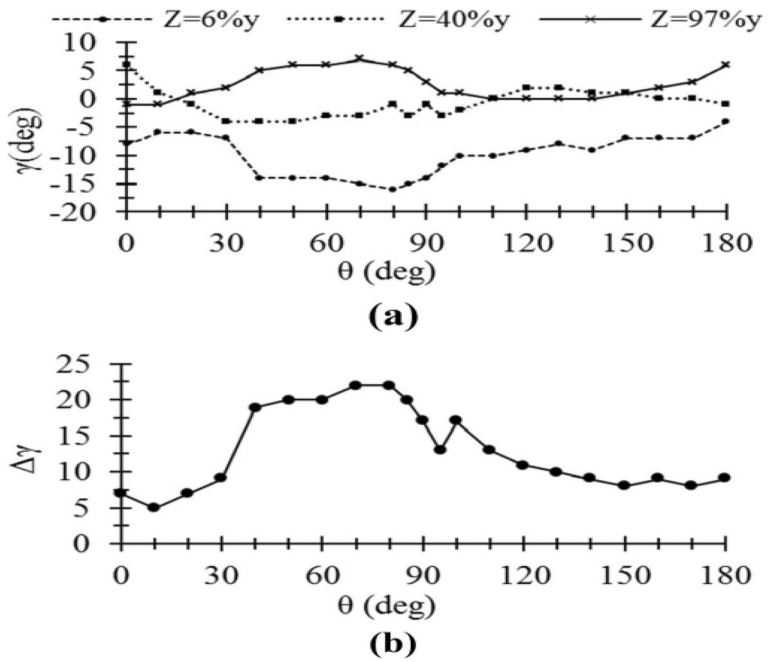

Fig. 13 **a** Flow deviation at different levels. **b** Difference of deviations for streams on channel bed relative to free surface

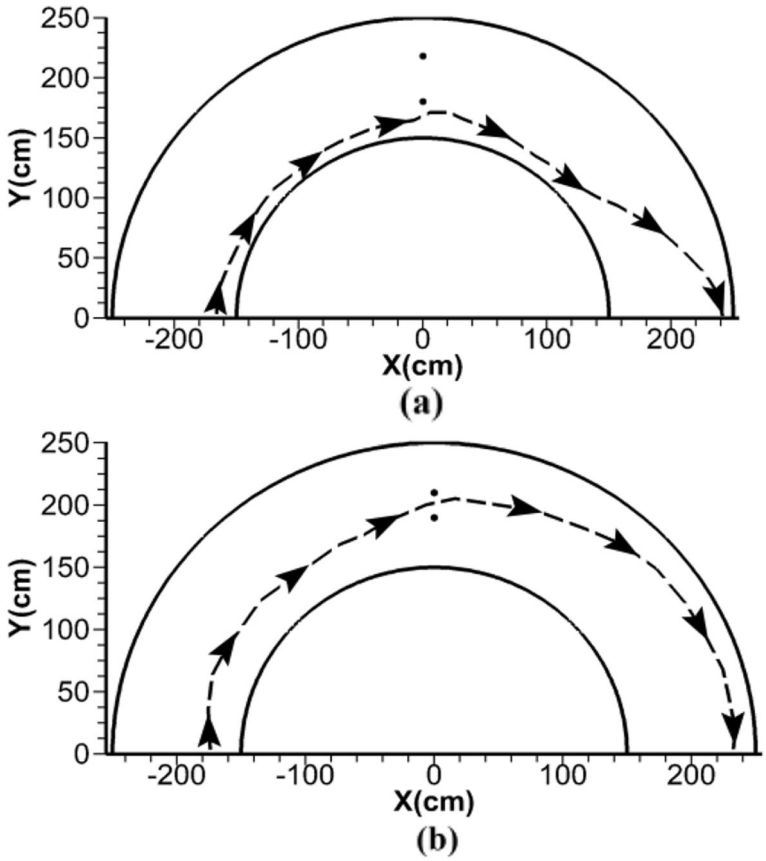

Fig. 14 Trajectory of maximum tangential velocity in (**a)** 6% and (**b)** 97% levels

transportation of particles from one layer to another, the induced vortex in the XZ plane would be convenient. The main cause of vortex generation in this region is the differences in tangential velocities for distinct levels. Flow tends to move in opposite directions in upper levels, while it would not happen for deeper levels. These differences in total fluid behavior would cause the vortex generation. However, it should be noted that opposite direction currents are mainly due to piers that prevent the flow. Considering the geometry of the piers and its influence on moving fluid against obstacles and rigid bodies, the flow tends to change its direction towards the pier, and the stream would be more parallel to pier boundaries. The reverse flow would be generated by an encounter of flows reaching each other from two sides of the pier. More hydrodynamic pier shapes can weaken the reverse flow considerably (Shafai [32]).

Shukry [33] introduced a so-called parameter "power of secondary flow" that is defined as the ratio of lateral flow kinetic energy to the total kinetic energy of the main flow [35]. The secondary flow strength is shown in Fig. 15. In this research, the maximum secondary flow occurs in the 92° section, due to the bend's twin pier at 90°. The amount of power of secondary flow is not considered at the initial stages and is not more than 2%. Suddenly, the secondary flow increases in 83° section and again declines to its initial value at approximately 100° section. The power of secondary flow is very considerable in 88 to 95° sections, and even it reaches over 8%. According to the streamlines drawn for different sections, it could be concluded that more vortexes are generated downstream of the piers. Moreover, the piers have a more significant influence downstream. However, there have been few changes in the secondary flow power in this case. The flow circulates in a spiral manner for bending paths. In such cases, a useful parameter called vorticity that is defined by velocity vector curl is defined. Vorticity would be equal to zero for irrotational flow. Vorticity is calculated along the bend and is represented in Fig. 16.

According to the above figure, vorticity values are much lower at the pier downstream when compared to those at the pier upstream. There are so many contra-rotating vortexes on the pier downstream that they cancel each other while there are only two vortexes upstream of the piers. The main secondary flow covers a great portion upstream, and hence the vorticity would be higher in this region. Maximum vorticity values occur

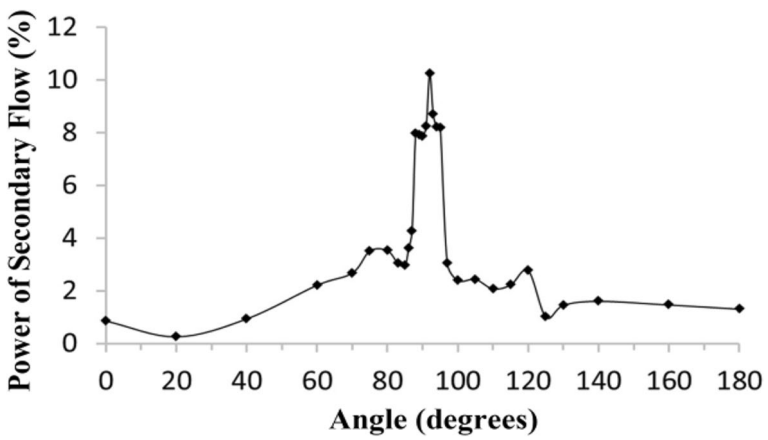

Fig. 15 Secondary flow intensities for different angles of the bend

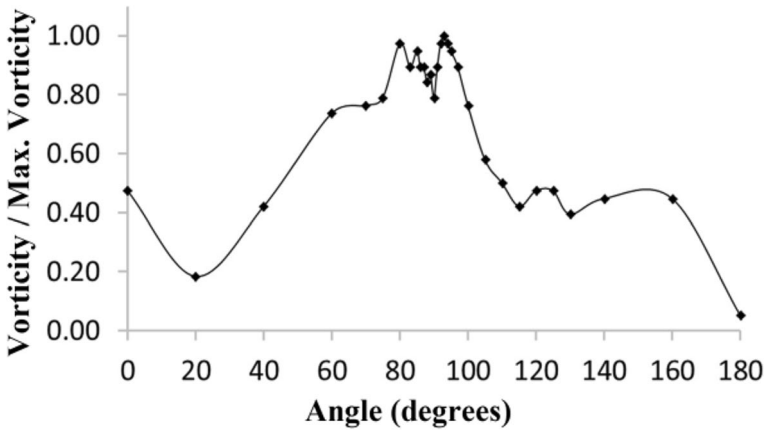

Fig. 16 The ratio of vorticity to maximum vorticity along the bend

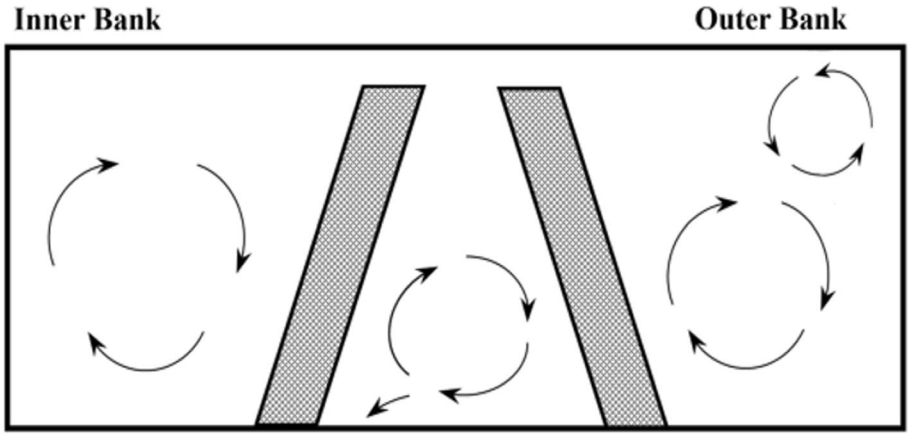

Fig. 17 Schematic of flow pattern around convergent twin pier in a plane normal to current

at the 80° section before the piers and 92° section downstream of the piers. The described process is similar to increasing and decreasing the vorticity in a 180° sharp bend without a pier [35].

Interaction of main secondary flow and twin piers are shown schematically in Fig. 17. The influencing range of bridge piers from the vortex generation point of view is proposed and shown in Fig. 18.

Conclusions

In this paper, a flow pattern along sharp 180° bend with twin convergent piers arranged normal to the flow is studied. The main findings of the research are summarized in the following:

1. Lateral flow is generated in bends more than the main secondary flow observed adjacent to the outer bank.

2. The main secondary flow is the major cause of the deviation of streamlines from the original trajectory of the bend. According to the defined parameter in this paper, flow

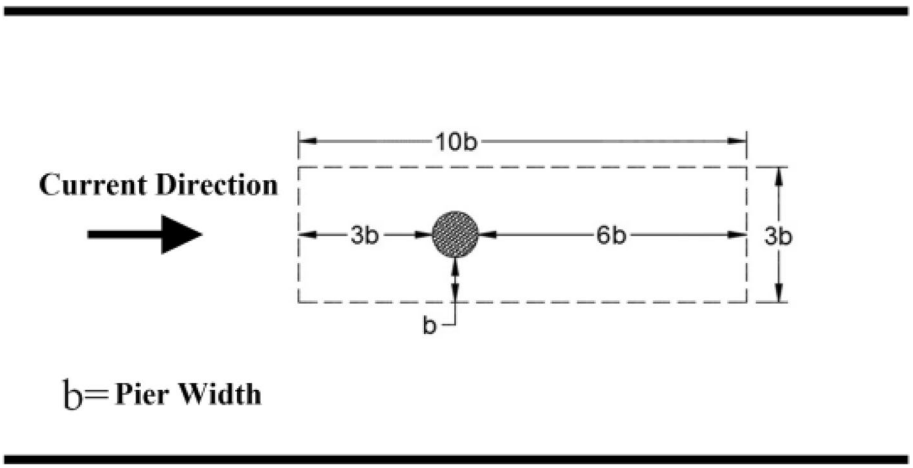

Fig. 18 Influencing range of piers on the flow pattern

deviation is negative near the bed and positive when approaching the free surface. The maximum recorded deviation is 22° for the section at 80° from the beginning of the bend.

3. Negative velocities were reported for all depths on the pier downstream. These negative velocities reached their maximum values at the free surface.

4. It is recommended to focus on this range in any further experimental attempts or numerical analysis. Moreover, the equivalent width should be considered when twin piers are applied.

Abbreviations

Rc	Central radius of channel
B	Channel with
Z	Distance to the channel bottom
U	Tangential velocity component
Θ	Angle from the beginning of the bend
X	Component X in the Cartesian coordinate system
Y	Component X in the Cartesian coordinate system
γ	Deviation angle
b	Pier with

Acknowledgements
Not applicable.

Authors' contributions
The authors declare that they have contribution in the preparation of this manuscript. All authors read and approved the final manuscript.

Funding
The authors received no funding for this work.

Availability of data and materials
All data generated or analyzed during this study are included in this published article**.**

Declarations

Competing interests
The authors declare that they have no competing interests.

Received: 23 December 2021 Accepted: 8 June 2022
Published online: 29 June 2022

References

1. Ahmed F, Rajaratnam N (1998) Flow around bridge piers. J Hydraul Eng 124(3):288–300. https://doi.org/10.1061/(ASCE)0733-9429(1998)124:3(288)
2. Akbari M, Vaghefi M (2017) Experimental investigation on streamlines in a 180° sharp bend. Acta Scientiarum Technol 39(4):425–432. https://doi.org/10.4025/actascitechnol.v39i4.29032
3. Akbari M, Vaghefi M, Chiew YM (2021) Effect of T-shaped spur dike length on mean flow characteristics along a 180-degree sharp bend. J Hydrol Hydromech 69(1):98–107. https://doi.org/10.2478/johh-2020-0045
4. Anderson S, Lohrmann A (1995) Open water test of the SonTek acoustic Doppler velocimeter. Proceedings of the IEEE Fifth Working Conference on Current Measurement, St. Petersburg, pp 188–192. https://doi.org/10.1109/CCM.1995.516172
5. Asadollahi M, Vaghefi M, Tabibnejad Motlagh MJ (2019) Experimental and numerical comparison of flow and scour patterns around a single and triple bridge piers located at a sharp 180 degrees Bend. Scientia Iranica 27(5):1–14. https://doi.org/10.24200/sci.2019.5637.1391
6. Ataie-Ashtiani B, Aslani-Kordkandi A (2012) Flow field around side-by-side piers with and without a scour hole. Eur J Mech B/Fluids 36:152–166. https://doi.org/10.1016/j.euromechflu.2012.03.007
7. Ataie-Ashtiani B, Aslani-Kordkandi A (2013) Flow field around single and tandem piers. Flow Turbul Combust 90(3):471–490. https://doi.org/10.1007/s10494-012-9427-7
8. Barbhuiya AK, Dey S (2004) Turbulent flow measurement by the ADV in the vicinity of a rectangular cross-section cylinder placed at a channel sidewall. Flow Measure Instrument 15(4):221–237. https://doi.org/10.1016/j.flowmeasinst.2004.02.002
9. Behrouzi Z, Hamidifar H, Zomorodian MA (2021) Numerical simulation of flow velocity around single and twin bridge piers with different arrangements using the Fluent model. Amirkabir J Civil Eng 53(9):15–15. https://doi.org/10.22060/CEEJ.2020.18136.6777
10. Blanckaert K, Graf WH (2001) Mean flow and turbulence in open-channel bend. J Hydraul Eng 127(10):835–847. https://doi.org/10.1061/(ASCE)0733-9429(2001)127:10(835)
11. Breusers HNC, Raudkivi AJ (1991) Scouring: Hydraulic structures design manual No. 2. Taylor and Francis, Rotterdam
12. Carnacina I, Leonardi N, Pagliara S (2019) Characteristics of flow structure around cylindrical bridge piers in pressure-flow conditions. Water 11(11):2240. https://doi.org/10.3390/w11112240
13. Chooplou CA, Vaghefi M (2019) Experimental study of the effect of displacement of vanes submerged at channel width on distribution of velocity and shear stress in a 180 degree bend. J Appl Fluid Mech 12(5):1417–1428. https://doi.org/10.29252/jafm.12.05.29329
14. Das R, Das S, Jaman H, Mazumdar A (2019) Impact of upstream bridge pier on the scouring around adjacent downstream bridge pier. Arab J Sci Eng 44(5):4359–4372. https://doi.org/10.1007/s13369-018-3418-5
15. Das S, Das R, Mazumdar A (2013) Circulation characteristics of horseshoe vortex in scour region around circular piers. Water Sci Eng 6(1):69–77
16. Das S, Mazumdar A (2018) Evaluation of hydrodynamic consequences for horseshoe vortex system developing around two eccentrically arranged identical piers of diverse shapes. KSCE J Civil Eng 22(7):2300–2314. https://doi.org/10.1007/s12205-017-1842-9
17. Dey S, Sarkar S, Fang H, Gaudio R (2018) Self-similarity in turbulent wall-wake flow downstream of a wall-mounted vertical cylinder. J Hydraulic Eng 144(6):04018023. https://doi.org/10.1061/(ASCE)HY.1943-7900.0001457
18. Fael C, Lança R, Cardoso A (2016) Effect of pier shape and pier alignment on the equilibrium scour depth at single piers. Int J Sediment Res 31(3):244–250. https://doi.org/10.1016/j.ijsrc.2016.04.001i
19. Gauton P, Eldho TI, Mazumdar BS, Behara MR (2019) Experimental study of flow and turbulence characteristics around simple and complex piers using PIV. Exper Thermal Fluid Sci 100:193–206. https://doi.org/10.1016/j.expthermflusci.2018.09.010
20. Graf WH, Istiarto L (2002) Flow pattern in the scour hole around a cylinder. J Hydraul Res 40(1):13–20. https://doi.org/10.1080/00221680209499869
21. Guan D, Chiew YM, Wei M, Hsich SC (2019) Characterization of horseshoe vortex in a developing scour hole at a cylindrical bridge pier. Int J Sediment Res 34(2):118–124. https://doi.org/10.1016/j.ijsrc.2018.07.001
22. Kumar A, Umesh C, Kothyari UC, Ranga Raju KG (2012) Flow structure and scour around circular component bride piers - A review. J Hydro Environ Res 6(4):261–265. https://doi.org/10.1016/j.jher.2012.05.006
23. Lee SO, Hong SH (2019) Turbulence characteristics before and after scour upstream of a scaled-down bridge pier model. Water 11(9):1900. https://doi.org/10.3390/w11091900
24. Liu Q, Tang H, Wang H, Xiao J (2018) Critical velocities for local scour around twin piers in tandem. J Hydrodynam 30(6):1165–1173. https://doi.org/10.1007/s42241-018-0122-6
25. Moghanloo M, Vaghefi M, Ghodsian M (2020) Experimental investigation on the effect of increasing the collar thickness on the flow pattern around the oblong pier in 180° sharp bend with balanced bed. J Appl Fluid Mech 13(1):245–260. https://doi.org/10.29252/jafm.13.01.30164
26. Naji Abhari M, Ghodsian M, Vaghefi M, Panahpur N (2010) Experimental and numerical simulation of flow in a 90-degree bend. Flow Measure Instrument 2(3):292–298. https://doi.org/10.1016/j.flowmeasinst.2010.03.002
27. Neill C. (1967). Mean-velocity criterion for scour of coarse uniform bed-material, 12th Congress of the International Association for Hydraulics Research, Colordo, USA.
28. Raudkivi AJ, Ettema R (1983) Clear-Water Scour at Cylindrical Piers. J Hydraul Eng 109(3):338–350
29. Salajegheh A, Salehi Neyshabouri AA, Ahmadi H, Mahdavi M, Ghodsian M (2005) An experimental investigation of three-dimensional flow pattern in river bend. Iran J Natural Resources 58(1):25–34 (In Persian)
30. Sarker MA (1998) Flow measurment around scoured bridge piers using Acoustic Doppler Velocimeter (ADV). Flow Measure Instrument 9(4):217–227. https://doi.org/10.1016/S0955-5986(98)00028-4
31. Sedighi F, Vaghefi M, Ahmadi G (2021) The effect of inclined pair piers on bed topography: clear water, incipient motion and live bed. Iran J Sci Technol Trans Civ Eng 45(3):1871–1890
32. Shafai BM (2013) Hydraulic of Sediment Transport, 2nd edn. Shahid Chamran University Press, Ahwaz in Persian
33. Shukry A (1950) Flow around bends in an open flume. Transact Am Soc Civil Eng 115:751–779

34. Vaghefi M, Akbari M, Fiouz AR (2015) Experimental investigation of the three-dimensional flow velocity components in a 180 degree sharp bend. World Appl Program 5(9):125–131
35. Vaghefi M, Akbari M, Fiouz AR (2016a) An experimental study of mean and turbulent flow in a 180 degree sharp open channel bend: Secondary flow and bed shear stress. KSCE J Civil Eng 20(4):1582–1593. https://doi.org/10.1007/s12205-015-1560-0
36. Vaghefi M, Ghodsian M, Salehi Neyshabouri AA (2009) Experimental study on 3D flow field around T shaped spur dike in a 90 degree bend. J Water Soil Conserv 16(2):105–130 (In Persian)
37. Vaghefi M, Ghodsian M, Salimi S (2016b) The effect of circular bridge piers with different inclination angles toward downstream on scour. Sadhana 41(1):75–86. https://doi.org/10.1007/s12046-015-0443-x
38. Vaghefi M, Ghodsian M, Salimi S (2016c) Scour formation due to laterally inclined circular pier. Arab J Sci Eng 41(4):1311–1318. https://doi.org/10.1007/s13369-015-1920-6
39. Vijayasree BA, Eldho TI, Mazumder BS (2020) Turbulence statistics of flow causing scour around circular and oblong piers. J Hydraul Res 58(4):673–686. https://doi.org/10.1080/00221686.2019.1661292
40. Vijayasree BA, Eldho TI, Mazumder BS, Ahmad N (2019) Influence of bridge pier shape on flow field and scour geometry. Int J River Basin Manage 17(1):109–129. https://doi.org/10.1080/15715124.2017.1394315
41. Wang L, Melville BW, Whittaker CN, Guan D (2018) Effects of a downstream submerged weir on local scour at bridge piers. J Hydro Environ Res 20:101–109. https://doi.org/10.1016/j.jher.2018.06.001
42. Yilmaz M, Yanmaz AM, Koken M (2017) Clear-water scour evolution at dual bridge piers. Can J Civil Eng 44(4):298–307. https://doi.org/10.1139/cjce-2016-0053

Publisher's Note